Effects of Shot Peening on Surface Mechanical Properties of Duplex Stainless Steel

F. Qiang, J. Chuanhai
1 School of Material Science and Engineering, Shanghai Jiao Tong University
H. PAN
EPCO Testing Technology (Shanghai) Ltd.

Abstract
Shot peening is a frequently used mechanical treatment to modify surface conditions of materials. The influence of shot peening on surface yield strength of S32205 duplex stainless steel has been investigated using X-ray stress analysis. Proof stresses $\sigma_{0.2}$ of both ferrite and austenite in the surface are enhanced after shot peening. Improvement on mechanical properties of modified surface was due to fine domain, high value of dislocation density induced by shot peening. Increment of proof stress $\sigma_{0.2}$ in austenite is larger than that of ferrite at same condition of SP, which is attributed to the easier domain size subdivision that is characterized by a higher harden-ability in austenite.

Keywords: Surface yield strength; Shot peening; Microstructure; Relaxation

Introduction

Duplex stainless steel (DSS) with a mixed structure of ferrite and austenite in approximately equal volume fractions combines many of beneficial properties of both phases, for example, it shows good resistance to oxidation, corrosion and stress corrosion associated with good mechanical properties [1 - 5]. Favorable mechanical properties of DSS are partly due to fine-grained structure, where grain growth is restricted by two phases to certain degree. However, tensile stresses are generated during manufacturing and following heat treatments, and fatigue properties of material are deteriorated. Moreover, compressive residual stresses are found in ferrite and balancing tensile residual stresses existing in austenite, and latter may deteriorate fatigue properties. To improve fatigue strength and fatigue life, surface mechanical treatments such as shot peening (SP) are employed to suppress crack initiation and growth at surface layers [6 - 8]. As an industrial important manufacturing process where material surface is plastic-elastically deformed by a stream of high velocity shot, SP usually introduces beneficial compressive residual stress (CRS) and microstructure refinements in material surface layers, which can improve material's fatigue resistance [9 - 11]. X-ray diffraction (XRD) is an important method to characterize residual stress and microstructure where effective penetration of X-ray beam is extremely shallow, generally about 10 μm in depth, diffracting volume can be considered to represent a free surface under plane stress [12, 13]. In a diffraction test, residual stress in such a thin surface layer usually exhibits a plane stress state [14], for one of the principal directions is vertical to surface plane with stress value close to zero. Under uniaxial load, residual stresses of surface are often biaxial. In most of previous work, only stress in loading direction was taken into account. In order to avoid the disadvantages mentioned above, in situ X-ray stress/strain analysis method has been put forward and applied [15-17]. During the tensile test, stresses of surface deformed by SP are in-situ measured by X-ray diffraction and applied strain is determined by strain gage techniques. Longitudinal and transverse directions are assumed to be principal directions of surface stress, thus, stresses normal to the specimen surface can be neglected. According to the Von Mises yielding criterion, only equivalent stress versus equivalent strain curve can properly characterize mechanical properties of specimen surface under biaxial stresses state [15]. The yield strength of surface can be determined according to stress-strain curve. It is well known that fatigue cracking normally initiates at surface, and cracks will not initiate or propagate in a compressively stressed

zone and the extent of mitigation depends strongly upon residual stress magnitude and distribution. The maximum CRS produced at or under surface of a part by SP treatment is at least as great as half yield strength of the peened material [18]. Unfortunately, any static or cyclic residual stress relaxation during component operation reduces achievable benefits. It is believed that improvement in fatigue properties depends mainly on the stability of residual stresses on tension-loaded state [19]. Although stress/strain in situ X-ray analysis method has been reported in Ref. [15- 17], little attention has been paid to shot-peened materials with two phases. Therefore, present work is devoted to study yield strength of both ferrite and austenite in S32205 DSS surface after SP treatments. In addition, relaxation behaviors of residual stress under static tensile loadings have also been investigated.

Experimental methods

S32205 DSS was supplied by Shanghai Bao-Steel Corporation with composition of C (0.021), S (0.001), Si (0.49), Mn (1.36), Cr (22.40), Ni (5.40), Mo (3.04), N (0.18), P (0.023), Cu (0.04), Al (0.004) and the rest Fe (all in wt. %). Specimen were cut into dog-bone shape with effective dimensions of 40 × 5 × 2 mm^3 then polished. Young's modulus of DSS 2205 is 205 GPa, yield stress is 460 MPa, and rupture strength is 625 MPa at room temperature. SP treatments were carried out on both sides of samples by an air blasting machine (Shanghai, Carthing Machinery Company). SP intensity was measured by arc height of Almen specimen (A type), which was controlled by jet pressure of nozzle, shot time and average ball diameter. Diameter of peening nozzle was 15 mm and distance between the nozzle and samples was 100 mm. SP coverage was 100% in all samples. Double SP were carried out in every shot type, where lower SP intensity and smaller balls were employed in secondary treatment compared with first one to smooth the surface. Shot media used in the first and second SP steps were cast steel balls with diameter of 0.6 mm (hardness 610 HV) and ceramic balls with diameter of 0.3 mm (hardness 700 HV), respectively. Shot time was 0.5 min for the first step and 0.3 min for second one. In present investigation, double SP treatments were carried out with SP intensities 0.17, 0.10 mmA, respectively. For tensile test, a micro-tensile tester (Shenzhen, Gopoint Testing Equipment Company) was used and standard tensile distance of the sample was 30 mm. Load along longitudinal direction was increased step by step with 50 MPa each time from 0 to 550 MPa with tensile rate of 1.0×10^{-3} /s. Original residual stress after SP, longitudinal stress σ_1 and transverse stress σ_2 under different loadings were analyzed with in-situ X-ray diffraction using $\sin^2\Psi$ method. Stresses of austenite {311} were measured on X-ray stress analyser (LXRD Proto, Canada) with Mn-Kα radiation (30 kV, 25 mA). Simultaneity, X-ray stress analyser (LXRD Proto, Canada) with Cr-Kα radiation was employed to check ferrite {211} samples (30 kV, 25 mA).

Results and discussions

Fig. 1 shows X-ray diffraction patterns of S32205 DSS before and after SP, and peaks have been indexed. Though no appreciable change in peak positions is found, both peak broadening and peak-asymmetry of DDS reflections increase after SP treatment in top surface. Diffraction peaks of shot-peened samples become wider, which results from smaller domain sizes and higher micro-strain [20]. In the process of SP, impact of small shot balls with high kinetic energy on the surface of samples causes elastic–plastic deformation and domain size refinement at surface layers [21].

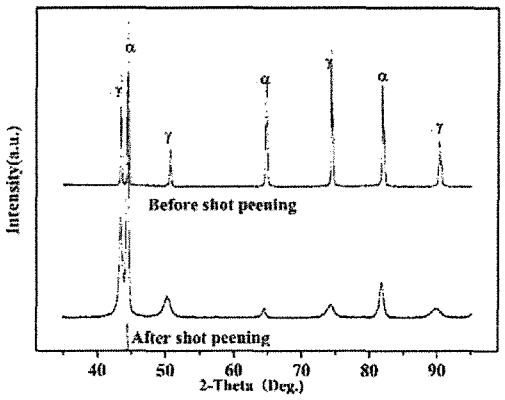

Fig. 1 XRD pattern of S32205 DSS before and after shot peening.

As mentioned in the introduction, longitudinal and transverse directions of plate specimen are two principal directions of biaxial residual stress in the surface. When external stress is applied in longitudinal directions, surface stress state is still biaxial and the principal directions do not change. According to Von Mises yielding criterion [14, 15], under biaxial stress state, surface equivalent stress $\overline{\sigma}$ under each load can be expressed as

$$\overline{\sigma} = \sqrt{\sigma_1^2 - \sigma_1\sigma_2 + \sigma_2^2} \quad (1)$$

Where σ_1, σ_2 denotes stress in longitudinal and transverse directions measured by in-situ X-ray stress analyzer, respectively. In elastic deformation stage, uniaxial equivalent strain $\overline{\varepsilon}$ is determined as

$$\overline{\varepsilon} = \varepsilon_e = \overline{\sigma} / E \quad (2)$$

in plastic deformation stage

$$\overline{\varepsilon} = \varepsilon_e + \varepsilon_P \quad (3)$$

Where E is Young's modulus, ε_e is elastic strain and ε_P is plastic strain $\overline{\sigma}', \overline{\sigma}'', \sigma_1', \sigma_1'', \sigma_2', \sigma_2'', \varepsilon_a', \varepsilon_a''$ denote surface equivalent stress, measured stress in longitudinal and transverse directions and applied strain of two adjacent measurement points in plastic deformation zone, respectively. The increment of equivalent plastic strain $\Delta\varepsilon_p$ for all points in plastic deformation zone can be determined as

$$\Delta\varepsilon_p = [(\overline{\sigma}' + \overline{\sigma}'')/|\sigma_1' + \sigma_1'' - (\sigma_2' + \sigma_2'')/2|]\,|\Delta\varepsilon_a - (\Delta\sigma_1 - \nu\Delta\sigma_2)/E| \quad (4)$$

Where $\Delta\sigma_1 = \sigma_1'' - \sigma_1', \Delta\sigma_2 = \sigma_2'' - \sigma_2', \Delta\varepsilon_a = \varepsilon_a'' - \varepsilon_a'$. Using this method, total equivalent plastic strain ε_p for every point in the plastic zone can be obtained.

The primary stresses σ_1, σ_2 are along longitudinal and transverse directions, respectively, measured by original residual stresses before external loading. Under uniaxial tensile, relationships between σ_1, σ_2 and ε_a for both ferrite and austenite in S32205 DSS surface layers without SP treatment are shown in Fig. 2 (a) and (b). For each, the point indicated by arrow is regarded as the boundary between elastic and plastic stage. From the data in $\sigma_1 - \varepsilon_a$ relationship of elastic stage, Young's modulus E can be obtained by linear regression, which is equal to the slope of regression

line, and E of ferrite and austenite is 210 ± 2 and 196 ± 2 GPa, respectively. It is well known that the E value of S32205 (205 GPa) is between the E value of ferrite and austenite. In plastic stage, the relationship curve of $\sigma_1 - \varepsilon_a$ is deviated from liner behaviors. Variations of transverse stresses σ_2 of both ferrite and austenite are not obvious during the uniaxial tension. According to the method described above and data in Fig. 2 (a) and (b), relationships between equivalent stress $\overline{\sigma}$ and uniaxial equivalent strain $\overline{\varepsilon}$ are obtained for ferrite and austenite, as shown in Fig. 3 (a) and (b). The proof stress $\sigma_{0.2}$ corresponding to the permanent plastic strain of 0.2% is shown with dash lines, and $\sigma_{0.2}$ of ferrite and austenite surface is 421 and 502 MPa, respectively, which are higher than those of same constituent [22].

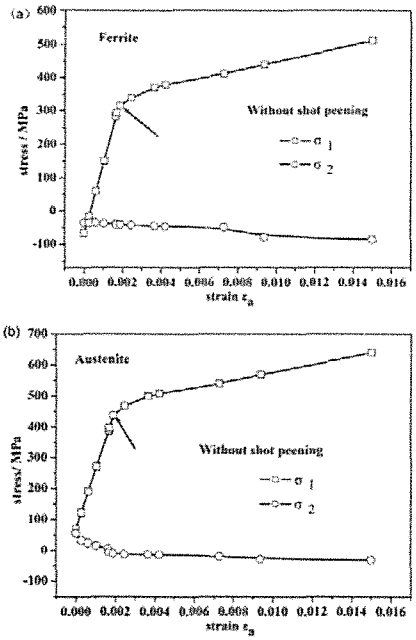

Fig. 2

Fig. 2 Variation of longitudinal (σ_1) and transverse stresses (σ_2) for unpeened specimen due to the applied tensile strain ε_a (a) ferrite, (b) austenite.

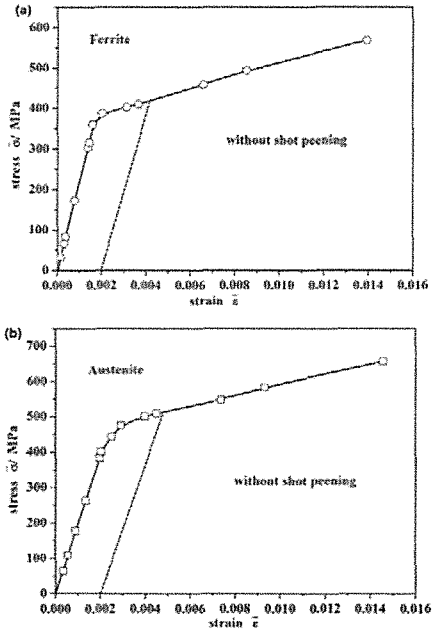

Fig. 3

Fig. 3 Relationships between the equivalent stress ($\overline{\sigma}$) and the equivalent uniaxial strain $\overline{\varepsilon}$ for unpeened specimen under the tensile load (a) ferrite, (b) austenite.

Before SP, benefitial mechanical properties of S32205 DSS are partly due to fine-grained structure since the grain growth is effectively suppressed due to two phases aggregated microstructure. An empirical formula proposed by Ashby et al. [23] to express relationship between material yield strength (σ_s) and micro-hardness (HV) (σ_s = 1/3×HV) shows micro-hardness is also related to material microstructure. High yield strength σ_s corresponds to high micro-hardness. It can be obtained that austenite has higher micro-hardness than ferrite as S32205 DSS in present research has a nitrogen content of 0.18 wt% in total, which is higher than 0.12 wt% as reported in the Ref [24]. Nitrogen has a low solubility in ferrite and it is mainly concentrated in austenite. Therefore,

addition of nitrogen in S32205 DSS increases hardness and yield strength of austenite. For shot-peened samples, original residual stresses along longitudinal and transverse directions without external load are employed as primary stress σ_1, σ_2, respectively. Before loading, primary compressive residual stresses is about -716 Mpa in ferrite, -798 Mpa in austenite with SP intensity of 0.17 + 0.10 mmA, respectively. Stress variations in longitudinal σ_1 and transverse σ_2 directions under loading as a function of applied strain ε_a at these two SP intensities are displayed in Fig. 4 respectively. It can be seen that with the increase of external load, the stress measured in longitudinal direction σ_1 is compressive stress and it decreases with increment of strain ε_a for both ferrite and austenite in elastic region, it then gradually changed to tensile stress in plastic region. However, σ_2 in transverse direction changed slightly at first and the variation is not obvious during uniaxial tension. Even with an external load of 550 MPa, σ_2 is still a compressive stress. In both ferrite and austenite under SP treatments, points indicated by arrows are regarded as boundary between plastic and elastic region [25]. Results show that slopes of ferrite and austenite are 210 ± 2 and 196 ± 2 GPa, respectively, which are approximate to the Young's modulus E of the bulk S32205 DSS with no SP treatment. In plastic region, curves of $\sigma_1 - \varepsilon_a$ in both ferrite and austenite are deviated from liner behaviors, which is similar to the results obtained before external loading as shown in Fig. 2. Based on the given method and data in Fig. 4, relationships between equivalent stress $\bar{\sigma}$ and uniaxial equivalent strain $\bar{\varepsilon}$ of shot-peened surface layer under different SP treatments are presented in Fig. 5. As shown in Fig. 5 (a), proof stress $\sigma_{0.2}$ corresponds to permanent plastic strain of 0.2%, and it is 935 MPa in ferrite under a SP intensity of 0.17 + 0.10. Correspondingly, $\sigma_{0.2}$ in austenite is 1158 MPa, as shown in Fig. 5 (b). Comparing to the proof stress of bulk S32205 DSS (421Mpa of ferrite and 502 MPa of austenite) without SP, proof stress of shot-peened surface increases 514 MPa in ferrite, and 656 MPa in austenite with SP treatment under an intensity of 0.17 + 0.10 mmA. The results indicate that increment of the proof stress $\sigma_{0.2}$ in austenite is more than that of ferrite under the same condition of SP. It can be easily obtained from above data that proof stresses in both ferrite and austenite are in proportion to compressive residual stress after SP. Surface compressive residual stresses are important in blocking crack initiation and initial propagation, and hardness is resistance to local plastic deformation [26], therefore, hardness is closely related to compressive residual stresses. The higher the compressive residual stresses are, the higher the hardness is, higher proof stresses are obtained as a result. After SP, the mechanical properties of metallic materials depend not only on residual stress but also on their microstructure. Comparing with ferrite, domain size of austenite is easier to subdivide in the process of SP, which is characterized by a higher harden-ability [20, 27]. This may be the reason why domain size and yield stress in austenite change obviously at the same SP condition. Simultaneously, the micro-strain variation is larger of austenite than that of ferrite after SP [27]. Different micro-strain variations between ferrite and austenite can be regarded as another reason why yield strengthen in austenite is larger than that in ferrite. Micro-strain is heightened sharply in the processing of SP, resulting in high dislocation density in the microstructure-changed layer. This change of microstructure makes dislocations hard to move in microstructure-changed layer or blocks the dislocation slip movements on the interface. Therefore, this microstructure change can increase fatigue life of shot-peened components [20].

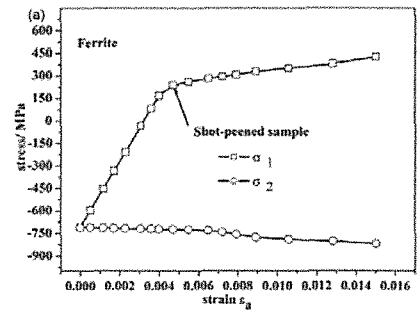

Fig. 4: Stress variation in longitudinal (σ_1) and transverse (σ_2) direction for shot peened specimen as a function of the ap-

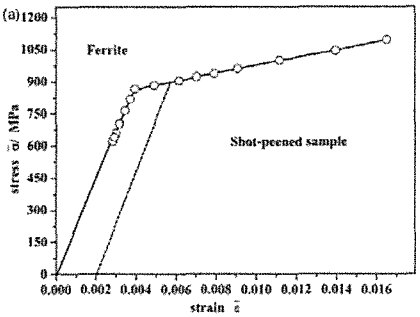

Fig. 5: Relationships between equivalent stress ($\bar{\sigma}$) and equivalent uniaxial strain $\bar{\varepsilon}$ for shot peened specimen under tensile load (a) ferrite, (b) austenite.

Conclusions

In-situ X-ray stress analysis for determining surface yield strength has been used to investigate the influence of SP on surface mechanical properties of S32205 DSS. The higher the compressive residual stress, the higher proof stress can be obtained both in ferrite and austenite after SP. Proof stress $\sigma_{0.2}$ variation in the surface of austenite is larger than that of ferrite, which can be attributed to easier domain size subdivision that is characterized by higher harden-ability in austenite. The results show that compressive residual stress, refined domain size, and high dislocation density in surface layer after SP lead to improved yield strength.

References

1. Itman Filho, J.M.D.A. Rollo, R.V. Silva, G. Martinez. Mater Lett. 59 (2005) 1192-1194.
2. Gurrappa, C.V. Krishna Reddy. J. Mater. Process Technol. 182 (2007) 195-201.
3. C.M. Garzon, A.P. Tschiptschin. Mater Sci Eng A. 441 (2006) 230-238.
4. Deng, Y. Jiang, J. Xu, T. Sun, J. Gao, L. Zhang, W. Zhang, J. Li. Corros Sci. 52 (2010) 969-997.
5. J.M. Cabrera, A. Mateo, L. Llanes, J.M. Prado, M. Anglada. J Mater Process Technol. 143-144 (2003) 321-325.
6. Y.F. Al-Obaid. Mech Mater. 19 (1995) 251-260.
7. S.B. Mahagaonkar, P.K. Brahmankar, C.Y. Seemikeri. Int J Adv Manuf Technol. 38 (2008) 563-574.
8. W. Luan, C. Jiang, V. Ji, Y. Chen, H. Wang. Mater Sci Eng A. 497 (2008) 374-377.
9. R. Menig, L. Pintschovius, V. Schulze, O. Vöringer. Scripta Mater. 45 (2001) 977-983.

10. M. Kobayashi, T. Matsui, Y. Murakami. Int J Fatigue. 20 (1998) 351-357.
11. S.P. Wang, Y.J. Li, M. Yao, R.Z. Wang. J Mater Process Technol. 73 (1998) 64-73.
12. B.E. Warren, X-ray Diffraction, Addison-Wesley, MA, 1969.
13. P. Virmoux, G. Inglebert, R.Gras., Dissipative Processes in Tribology, D. Downson et al. eds., Elsevier Science B V 27 (1994) 287-301.
14. W.L. Luan, C.H. Jiang, V. Ji. J Mater Sci. 44 (2009) 2454-2458.
15. Ma, K. Xu, J. He, J. Lu. Surf Coat Technol. 116-119 (1999) 128-132.
16. A.C., Batista, A., Dias. J of Test Eval. 28 (2000) 217-223.
17. W.Z. Luan, C.H. Jiang and V. Ji, Mater. Trans. 50, (2009) 158-160.
18. A.T. Ozdemir, L. Edwards, Fatigue Frucr. Eng. Mater.Struct. 1997, 20, 1443- 1451.
19. T. Roland, D. Retraint, K. Lu, J. Lu, Scr. Mater. 2006, 54, 1949-1954.
20. J. Langford. J Appl Crystallogr 11 (1978) 10-14.
21. Q. Feng, X. Wu, C. Jiang, Z. Xu, K. Zhan, Nucl Eng Des 255 (2013) 146-152.
22. J.O. Nilsson, Mater Sci Technol. 8 (1992) 685-700.
23. M. Ashby, D. Jones, Engineering Materials I, Per-gamon, Oxford, 1984.
24. J. Johansson, M. Odén, X.-H. Zeng. Acta mater. 47 (1999) 2669-2684.
25. B. Scholtes, E. Macherauch. Z Metallkd 77 (1986) 322-326.
26. G.E. Dieter, Mechanical Metallurgy, McGraw-Hill, New York, USA, 1961.
27. Q. Feng, C. Jiang, Z. Xu, Mater. Design. 47 (2013) 68-73.